Controllable Synthesis of TiO2 Single Crystals with Tunable Shapes Using Ammonium-Exchanged Titanate Nanowires as Precursors

ARTICLE *in* CRYSTAL GROWTH & DESIGN · APRIL 2010

Impact Factor: 4.89 · DOI: 10.1021/cg9012087

5 AUTHORS, INCLUDING:

Jianming Li
Peking University
16 PUBLICATIONS **659** CITATIONS
SEE PROFILE

Jingjian Li
Peking University
32 PUBLICATIONS **512** CITATIONS
SEE PROFILE

DOI: 10.1021/cg9012087

CRYSTAL GROWTH & DESIGN Article

2010, Vol. 10
2111–2115

Controllable Synthesis of TiO_2 Single Crystals with Tunable Shapes Using Ammonium-Exchanged Titanate Nanowires as Precursors

Jianming Li, Yuxiang Yu, Qingwei Chen, Jingjian Li, and Dongsheng Xu*

Beijing National Laboratory for Molecular Sciences, State Key Laboratory for Structural Chemistry of Unstable and Stable Species, College of Chemistry and Molecular Engineering, Peking University, Beijing 100871, People's Republic of China

Received October 2, 2009; Revised Manuscript Received March 15, 2010

ABSTRACT: A novel type of titanium precursor, ammonium-exchanged titanate nanowires, is used to hydrothermally synthesize nanosized TiO_2 single crystals with well-defined facets. With additives of appropriate shape-capping reagents, octahedral, truncated octahedral, and spindle-like TiO_2 nanocrystals have been obtained. We proposed that the transformation mechanism from ammonium-exchanged titanate nanowires to TiO_2 may be a "dissolution−nucleation" process. Furthermore, the photocatalytic activities of anatase TiO_2 nanocrystals with different facets exposed have been investigated.

Introduction

The synthesis of inorganic nanocrystals with well-defined shapes has attracted extraordinary attention due to the importance of surface structure of materials in determining their properties. In particular, the catalytic activity depends greatly on the arrangement of surface atoms and the numbers of dangling bonds on different crystal facets, and catalysts exposed with high-index or high-energy facets in general tend to exhibit high catalytic activity. TiO_2 is one of the most studied oxide semiconducting materials due to its low cost, nontoxicity, stability, and wide uses in photocatalysts, photosplitting water, dye-sensitized solar cells, photochromic devices, and gas sensing.[1−5] Recently, anatase TiO_2 single crystals with a high percentage of {001} facets were formed by using hydrofluoric acid as a morphology-controlling agent in TiF_4 aqueous solution[6−8] or by a nonaqueous synthetic route.[9]

A variety of wet chemical routes, including sol−gel,[10−12] nonaqueous sol,[9,13,14] hydro-/solvothermal method,[15−21] and other techniques,[4] have been developed to prepare TiO_2 nanocrystals. Among them, choosing a suitable titanium precursor with a proper transformation process is very important because it can directly influence the phases, sizes, shapes, and exposed facets of TiO_2.[10−21] Titanium alkoxides and titanium tetrachloride are widely used as titanium precursors, but the available precursors exhibit high reactivity which invariably leads to a mixture of different polymeric species.[4] Although the hydrolysis rates can be controlled when using alcohol or chelating agents such as dihydric alcohol or carboxylic acid,[22−27] the obtained TiO_2 seldom exhibits specific facets in a relatively high yield. Meanwhile, the evaporation of organic molecules would cause environmental pollution.[17] Therefore, it is necessary to find a new titanium precursor to selectively prepare TiO_2 with tunable shapes and expose specific facets as well as producing little environmental pollution.

Titanate nanofibers derived from the alkali treatment of TiO_2 nanoparticles under a highly basic condition are considered as a potential precursor for preparing TiO_2. By exchanging alkali ions with protons to form the H-titanate, thermal dehydration reactions at high temperature[28,29] or hydrothermal treatments[15,16,30,31] under a neutral or an acidic condition are conducted in an attempt to cause bond cleavage and, thus, destruction of the fibers. We and Wong et al. have demonstrated that a shape-dependent morphological transformation occurred during the hydrothermal chemical transformation, in neutral solution, of H-titanate nanostructures into their anatase titania counterparts.[15,16] However, TiO_2 nanocrystals prepared by hydrothermal transformation of titanate nanowires are limited to a mixture of nanoscale cubes and rhombohedra.[16] Herein, we demonstrated that ammonium-exchanged titanate nanowires (ATNWs) could be used as a precursor to prepare nanosized TiO_2 with well-defined facets.

Experimental Section

Preparation of Ammonium-Exchanged Titanate Nanowires (ATNWs):. Potassium titanate nanwires (KTNWs) were prepared by hydrothermal reaction of P25 in KOH solution.[32] Typically, 2 g of P25 was dispersed in 80 mL of 10 M KOH solution and placed into a 100 mL Teflon-lined autoclave. The autoclave was heated at 200 °C for 24 h, and then naturally cooled to room temperature, producing white $K_2Ti_6O_{13}$ precipitates. These white precipitates were isolated from solution by centrifugation and subsequently washed with deionized water several times until the pH of the solution was less than 10. The ATNWs were prepared by ammonium ion-exchange of the KTNWs in 0.1 M NH_4NO_3 solution with agitating for several hours and then isolated by centrifugation. This step was repeated several times. The obtained ATNWs were washed with deionized water several times and then dried at 60 °C in vacuum for 10 h.

Synthesis of TiO_2 Nanocrystals with Different Shapes:. In a typical experiment, 0.2 g of ATNWs was dispersed in 40 mL of deionized water and placed into a 50 mL Teflon-lined autoclave. The autoclave was heated at 200 °C for 24 h. After naturally cooling to room temperature, the obtained white TiO_2 precipitates were isolated from solution by centrifugation and subsequently washed with deionized water and ethanol.

Material Characterization:. The morphologies and the structures of the samples were characterized by scanning electron microscopy (SEM, Zeiss Supra-55), transmission electron microscopy (TEM), and high-resolution TEM (HRTEM, FEI Tecnai F30 with 300 kV),

*To whom correspondence should be addressed. E-mail: dsxu@pku.edu.cn. Phone: 86-10-62753580. Fax: 86-10-62760360.

Published on Web 04/20/2010

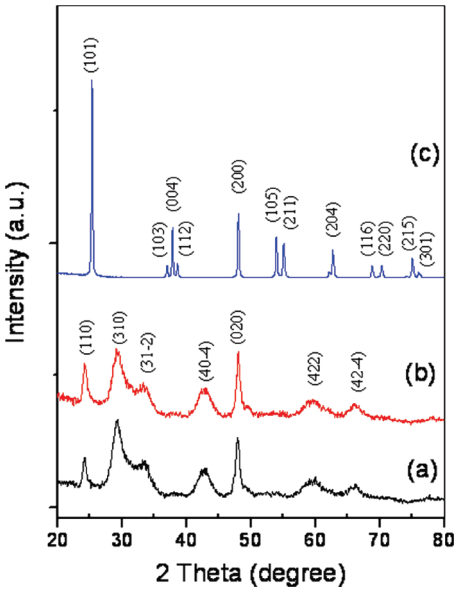

Figure 1. X-ray diffraction patterns: (a) KTNWs, (b) ATNWs, and (c) TiO_2 particles prepared by hydrothermal reaction of ATNW precursors in water.

X-ray powder diffraction (XRD, Rigaku D/max-2500 diffractometer with Cu Kα radiation, $\lambda = 0.1542$, 40 kV, 100 mA), and BET (Micrometrics ASAP 2010). X-ray photoelectron spectra (XPS) were analyzed on a Kratos Axis Ultra System with monochromatic Al Kα X-rays (1486.6 eV), operated at 14 V and 14 mA (emission current) in a chamber with a base pressure of approximately 10^{-8} Pa.

Photocatalytic Measurement:. Photocatalytic reactions for decomposition of methylene blue (MB) were carried out on a Pyrex beaker with 9 cm in diameter and 5 cm in height. An 8 W U-type UV lamp with a maximum emission at 254 nm was used as the UV resource. Typically, 20 mg of TiO_2 particles was dispersed in 100 mL of 2.0×10^{-5} M methylene blue (MB) aqueous solution in an ultrasonic bath to form a suspension, and the suspension was magnetically stirred for 30 min in the dark. At regular irradiation time intervals, the dispersion was sampled and centrifuged to separate the TiO_2 particles. The residual MB concentration was detected using a Lambda 45 UV/vis spectrometer (Perkin-Elmer Instruments). For comparison, P25 was used as the standard sample for the photocatalytic activity.

Results and Discussion

As-prepared solid samples of both ammonium-exchanged titanate nanowires and anatase nanostructures were characterized by XRD. Most of the XRD peaks of the potassium titanate nanotubes (KTNWs) in Figure 1a might be identified with the $K_2Ti_6O_{13}$ structure (monoclinic, $C2/m$, JCPDS 40-0403), which matched well with other reports.[32,33] By exchanging the ammonium ion, the KTNWs were transferred to the ATNWs. Because the ionic radius of NH_4^+ is similar to that of K^+, the ion-exchange did not destroy the structure of the Ti−O−Ti networks. As seen in Figure 1b, all of the diffraction peaks of the ATNWs are similar to those of the KTNWs. XPS analysis showed a N/K/Ti/O molar ratio of 1:2:10:22 (see Figure S1 and Table S1 in the Supporting Information), indicating that only 33% K^+ ions in the KTNWs were exchanged by NH_4^+. After further hydrothermal treatment of the ATNW precursors in deionized water, a pure anatase phase of TiO_2 (tetragonal, $I4_1/amd$, JCPDS 21-1272) was observed, as shown in Figure 1c.

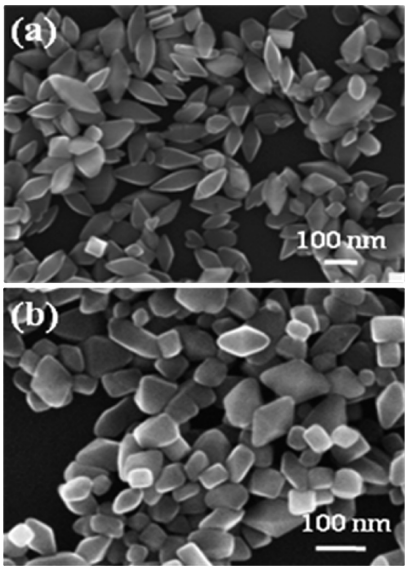

Figure 2. SEM image of TiO_2 particles prepared by hydrothermal reaction of ATNWs in pure water for 24 h at different temperatures: (a) 150 and (b) 200 °C.

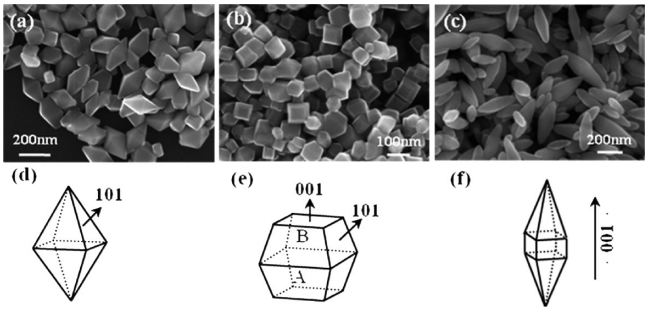

Figure 3. SEM images of TiO_2 particles prepared by hydrothermal reaction of ATNW precursors in (a) 0.05 M hexamethylenetetramine; (b) 0.1 M ammonium fluoride; (c) 0.1 M hexadecyltrimethylammonium bromide. (d−f) Schematic drawings of shapes of TiO_2 particles in panels a, b, and c, respectively.

Figure 2a displays the SEM images of the anatase sample prepared by hydrothermal treatment of the ATNWs in deionized water at 150 °C. A large quantity of octahedral particles with the sizes of 20−100 nm or longer octahedral with well-developed facets were observed. Increasing the temperature of the hydrothermal reaction would result in some round edges of the octahedra (Figure 2b), which might be attributed to the fast transformation rate from ATNWs to TiO_2.

Hexamethylenetetramine (HMTA), ammonium fluoride, and hexadecyltrimethylammonium bromide (CTAB) were used as capping reagents to control the shape of the TiO_2 nanocrystals. As shown in Figure 3a, with additive of 0.05 M HMTA, uniform octahedral TiO_2 nanocrystals with sharp edges were obtained in a relative high yield (>80%). In the case of 0.1 M ammonium fluoride as a capping reagent, most (above 90%) of the particles in Figure 3b exhibited truncated octahedra, which exposed high energy {001} facets. In order to define the degree of truncation, the edge lengths of the truncated octahedral TiO_2 crystal are labeled with A and B (Figure 3e), indicating that the ratio of B/A was about 0.60. Thus, the percentage of {001} facets was estimated to be approximately 17%. On the basis of the BET surface area of

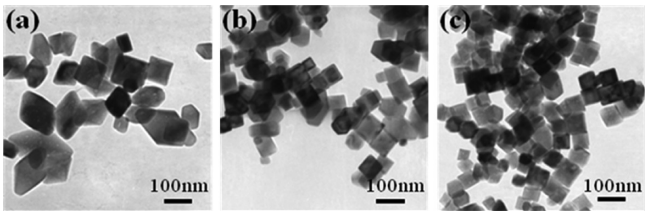

Figure 4. TEM images of TiO_2 particles prepared by hydrothermal reaction of ATNW precursors in (a) 0.05 M, (b) 0.1 M, and (c) 0.2 M ammonium fluoride.

28 $m^2 \cdot g^{-1}$ for the truncated octahedral samples by nitrogen sorptometer measurement, we can calculate that the total area of exposed {001} facets was about 4.8 $m^2 \cdot g^{-1}$, which was much larger than that of the reports by Yang et al.[7,8] Moreover, by using 0.1 M CTAB as a capping reagent, the products present a spindle-like morphology with sizes from tens to hundreds of nanometers (Figure 3c).

The quantities of capping reagents also affect the shape transformation from ATNWs to anatase TiO_2. Figure 4 show the TEM images of the products obtained from hydrothermal reaction of ATNWs in ammonium fluoride solutions with different concentrations at 200 °C for 24 h. Nanocrystals with a truncated octahedral structure were observed with the addition of 0.05 M ammonium fluoride (Figure 4a). At a higher concentration of ammonium fluoride, the truncation degree of the octahedra increased as the particle sizes became uniform (Figure 4b,c).

Figure 5 shows the TEM and HRTEM images of TiO_2 nanocrytals with different morphologies. As seen in Figure 5b, three sets of lattice space, 0.35, 0.35, and 0.48 nm, were observed in the octahedral crystal, which correspond to (101), (−101), and (002) of the anatase phase, respectively. From the corresponding fast Fourier transfer images (the inset of Figure 5b), the angle of (101) and (−101) was 43.4°, which was in agreement with the angle between plane (101) and plane (−101) calculated from the lattice constants of anatase (tetragonal space group $I4_1/amd$, $Z = 4$, $a = 0.37852$ nm, $c = 0.95139$ nm).[34] Thus, we can conclude that the predominantly exposed specific facets of the octahedral crystal were {101} facets. It is worth noting that, although theoretical calculation predicated that anatase TiO_2 nanocrystals are dominated by the thermodynamically stable {101} facets (more than 94% based on the Wulff construction[35,36]), preparing anatase TiO_2 nanocrystallites with mainly exposed {101} facets in a relatively high yield was still rarely reported.[20] For the truncated octahedral samples, as seen in Figure 5c, the interfacial angle between the truncated facet and the surrounding facet is 68.3°, which can be attributed to the angle between the {001} and {101} facets of anatase.[34] Also, the HRTEM image demonstrated that the truncated plane was (002) and the exposed facets were dominated by {101} and {001} facets (Figure 5d). In a spindle-like particle (Figure 5f), the crystal grew along the ⟨001⟩ direction.

Furthermore, a detailed time-dependent morphology evolution study was conducted in 0.05 M HMTA solution at 200 °C as an example to investigate the transformation process from ATNWs to TiO_2, as shown in Figure 6a−d. It was observed that more particles appeared and the particles gradually grew up while the diameter and length of ATNWs decreased along with hydrothermal reaction. When hydrothermal reaction time was longer than 12 h, the ATNWs would completely transfer to octahedral anatase particles.

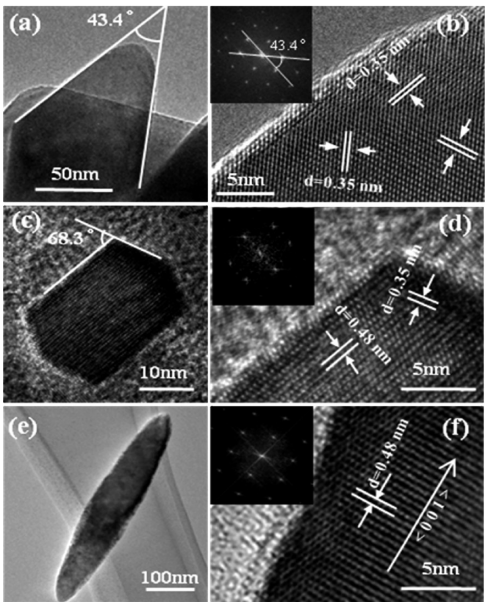

Figure 5. TEM image of three morphologies of TiO_2 taken from (a) octahedral, (c) truncated octahedral, and (e) spindle-like. (b,d,f) HRTEM images taken from panels a, c, and e, respectively. Insets are the corresponding fast Fourier transfer images.

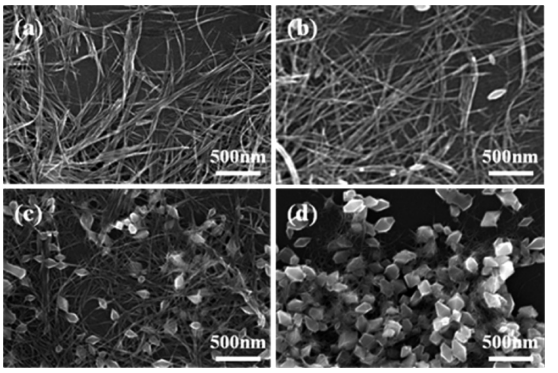

Figure 6. SEM image of TiO_2 particles prepared by hydrothermal reaction of ATNW precursors in 0.05 M hexamethylenetetramine with reaction times of (a) 0, (b) 1 h, (c) 3 h, and (d) 5 h.

In addition, we have measured the pH evolution of the solution during the transformation. At the beginning of the hydrothermal reaction, the pH of the solution containing 0.05 M HMTA was 8.4. After 3 and 12 h of the hydrothermal reaction, the pH values increased to 9.5 and 10.4, respectively. For other capping reagents, it was also found that the pH would gradually increase with the reaction time. If we varied the pH of the initial solution in a range of 6−9 by nitric acid or ammonia, no obvious change in the morphologies of the final products was observed.

Upon hydrothermal treatment of the ATNWs, the transformation would proceed with the dissolution and nucleation mechanism. At the beginning of the transformation, the surface of ATNWs gradually decomposed and produced $Ti(OH)_4$ fragments, ammonia, and potassium ions under hydrothermal conditions at higher temperature according to eq 1. Then, $Ti(OH)_4$ fragments were rearranged through a dehydration reaction between Ti−OH and HO−Ti in an edge-sharing manner, resulting in the formation of anatase crystal nuclei, according to eqs 2 and 3.

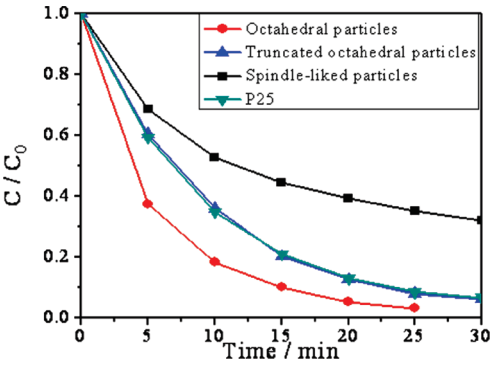

Figure 7. Photocatalytic activities of the samples with different morphologies and P25 for MB decomposition. The catalyst concentration was 0.2 g L^{-1}, and the initial concentration of MB was 2.0×10^{-5} mol L^{-1}.

Subsequently, the TiO_2 nuclei gradually grew up to form TiO_2 nanocrystals when $Ti(OH)_4$ fragments diffused to their surfaces. Due to anisotropy in adsorption stability of the capping reagents, the additives adsorbed onto a certain crystallographic plane more strongly than others, which lowers the surface energy of the bound plane and hinders the growth of crystals or some crystal planes. In the present system, we believe that F^- and CTAB would be adsorbed preferentially on the (001) and (100) surfaces of the anatase crystal and thus limited the crystal growth along the *c*-axis and the lateral surfaces, respectively.

Other transformation mechanisms, such as in-site transformation and topochemical reaction,[30] might undergo the dehydration and deammonium process when ATNWs converted to anatase, in which some N would be left in the TiO_2 crystal lattice and be N-doped. To eliminate this hypothesis, we measured the UV−vis diffuse reflectance spectra of TiO_2 particles prepared by hydrothermal treatment of the ATNWs in deionized water at 200 °C. All of the samples are white powder, in contrast to the yellow color of N-doped TiO_2,[37] and the absorption curves matched well with the band gap of pure anatase. In addition, no anatase was found in the products when ATNWs were treated in the an ethanol bath at 200 °C for 24 h.

In general, the catalytic activity of TiO_2 nanocrystals depends greatly on the arrangement of surface atoms and the numbers of dangling bonds on different crystal facets.[38−42] We have investigated the photocatalytic activity of the samples with morphologies, by photocatalytic oxidative decomposition of MB under UV irradiation as a test reaction (Figure 7). For comparison, the photocatalytic activity of Degussa P25, a widely used standard photocatalyst, is also given in Figure 7. It can be seen that octahedral particles exhibit the highest photocatalytic activity, and the photodecomposition rate could be sequenced as octahedral particles > truncated octahedral particles = P25 > spindle-like particles.

Table 1. BET Surface Area and Photocatalytic Properties of Different Morphologies and P25

morphologies	octahedral	truncated octahedral	spindle-like	P25
BET/m^2 g^{-1}	15	28	16	52
rates k/min^{-1}	0.15	0.11	0.04	0.10
$(k/S)/(k$P25/SP25)	5.2	2.0	1.3	1.0

To quantitatively calculate the photocatalytic activities of catalysts, we studied the kinetics of MB photodecomposition rates over the samples. The photodecomposition reaction approximately obeys the first-order kinetics, and the photocatalytic reaction can be simply described by $dC/dt = kC$, where C is the concentration of MB, and k denotes the overall degradation rate constant. The photocatalytic activity has been defined as the overall degradation rate constant of the catalysts. By plotting $\ln(C_0/C)$ as a function of time through regression, we obtained for each sample the k (min^{-1}) constant from the slopes of the simulated straight lines, as listed in Table 1. Surface area is one of the vital factors in determining the photocatalytic activity of the catalyst. The BET surface area of the products and P25 are also listed in Table 1. By using the normalized photocatalytic rates, which compared surface area, we found that the reaction rates of the samples with morphologies of octahedral, truncated octahedral, and spindle were 5.2, 2.0, and 1.3 times that compared to the Degussa P25, respectively. In our experiments, the sample with truncated octahedral morphology did not exhibit high photocatalytic activity, which might be because the high-energy {001} facets were terminated by fluorine atoms and the real surface energy could be sequenced as the F-001 < F-101 facet.[6] In addition, we proposed that the excellent photocatalytic activity of the anatase particles with a lower-energy {101} facet exposed may be attributed to their high crystallinity and few defects on the surfaces of the perfect crystals.

Conclusions

In summary, a novel type of titanium precursor, ammonium-exchanged titanate nanowires, was used to prepare nanosized anatase TiO_2 with well-defined facets using a hydrothermal method. Octahedral, truncated octahedral, and spindle-like TiO_2 particles have been synthesized by kinetically controlling the growth rates of various facets of TiO_2 particles with appropriate capping agents. We proposed that the transformation mechanism from ATNWs to TiO_2 may be a "dissolution−nucleation" process, which was different from the in-site transformation and topochemical reaction for other titanates. Studies on the photocatalytic activities of anatase TiO_2 nanocrystals with different facets exposed indicated that the reaction rates of the samples with

morphologies of octahedral, truncated octahedral, and spindle were 5.2, 2.0, and 1.3 times that compared to the Degussa P25, respectively. It is expected that this approach may provide a versatile, facile, and green pathway for designing TiO_2 nanostructures with novel morphologies.

Acknowledgment. This work is supported by NSFC (Grant Nos. 20525309, 20673008, 50821061) and MSTC (MSBRDP, Grant Nos. 2006CB806102, 2007CB936201).

Supporting Information Available: Additional table and figure. This material is available free of charge via the Internet at http://pubs.acs.org.

References

(1) Fujishima, A.; Honda, K. *Nature* **1972**, *238*, 37.
(2) Grätzel, M. *Nature* **2001**, *414*, 338.
(3) Barbe, C. J.; Arendse, F.; Comte, P.; Jirousek, M.; Lenzmann, F.; Shklover, V.; Grätzel, M. *J. Am. Ceram. Soc.* **1997**, *80*, 3157.
(4) Chen, X.; Mao, S. S. *Chem. Rev.* **2007**, *107*, 2891.
(5) O'Regan, B.; Grätzel, M. *Nature* **1991**, *353*, 737.
(6) Yang, H. G.; Sun, C. H.; Qiao, S. Z.; Zou, J.; Liu, G.; Smith, S. C.; Cheng, H. M.; Lu, G. Q. *Nature* **2008**, *453*, 638.
(7) Yang, H. G.; Liu, G.; Qiao, S. Z.; Sun, C. H.; Jin, Y. G.; Smith, S. C.; Zou, J.; Cheng, H. M.; Lu, G. Q. *J. Am. Chem. Soc.* **2009**, *131*, 4078.
(8) Han, X.; Kuang, Q.; Jin, M.; Xie, Z.; Zheng, L. *J. Am. Chem. Soc.* **2009**, *131*, 3152.
(9) Wu, B.; Guo, C.; Zheng, N.; Xie, Z.; Stucky, G. D. *J. Am. Chem. Soc.* **2008**, *130*, 17563.
(10) Chemseddine, A.; Moritz, T. *Eur. J. Inorg. Chem.* **1999**, 235.
(11) Sugimoto, T.; Zhou, X.; Muramatsu, A. *J. Colloid Interface Sci.* **2003**, *259*, 53.
(12) Moritz, T.; Reiss, J.; Diesner, K.; Su, D.; Chemseddine, A. *J. Phys. Chem. B* **1997**, *101*, 8052.
(13) Zhang, Z. H.; Zhong, X. H.; Liu, S. H.; Li, D. F.; Han, M. Y. *Angew. Chem., Int. Ed.* **2005**, *44*, 3466.
(14) Niederberger, M.; Bartl, M. H.; Stucky, G. D. *J. Am. Chem. Soc.* **2002**, *124*, 13642.
(15) Yu, Y.; Xu, D. *Appl. Catal. B* **2007**, *73*, 166.
(16) Mao, Y.; Wong, S. S. *J. Am. Chem. Soc.* **2006**, *128*, 8217.
(17) Wu, M.; Lin, G.; Chen, D.; Wang, G.; He, D.; Feng, S.; Xu, R. *Chem. Mater.* **2002**, *14*, 1974.
(18) Murakami, N.; Kurihara, Y.; Tsubota, T.; Ohno, T. *J. Phys. Chem. C* **2009**, *113*, 3062.
(19) Wang, D.; Liu, J.; Huo, Q.; Nie, Z.; Lu, W.; Williford, R.; Jiang, Y. B. *J. Am. Chem. Soc.* **2006**, *128*, 13670.
(20) Amano, F.; Yasumoto, T.; Prieto-Mahaney, O.-O.; Uchida, S.; Shibayama, T.; Ohtani, B. *Chem. Commun.* **2009**, 2311.
(21) Hosono, E.; Fujihara, S.; Kakiuchi, K.; Imai, H. *J. Am. Chem. Soc.* **2004**, *126*, 7790.
(22) Wang, C.-C.; Ying, J. Y. *Chem. Mater.* **1999**, *11*, 3113.
(23) Kumazawa, H.; Otsuki, H.; Sada, E. *J. Mater. Sci. Lett.* **1993**, *12*, 839.
(24) Kumar, K. P.; Kumar, J.; Keizer, K. *J. Am. Ceram. Soc.* **1994**, *77*, 1396.
(25) Yoldas, B. *J. Mater. Sci.* **1986**, *21*, 1087.
(26) Harris, M. T.; Byers, C. H. *J. Non-Cryst. Solids* **1988**, *103*, 49.
(27) Sanchez, C.; Livage, J.; Henry, M.; Babonneau, F. *J. Non-Cryst. Solids* **1988**, *100*, 65.
(28) Armstrong, A.; Armstrong, G.; Canales, J.; Bruce, P. *Angew. Chem., Int. Ed.* **2004**, *43*, 2286.
(29) Yoshida, R.; Suzuki, Y.; Yoshikawa, S. *J. Solid State Chem.* **2005**, *178*, 2179.
(30) Zhu, H.; Gao, X.; Lan, Y.; Song, D.; Xi, Y.; Zhao, J. *J. Am. Chem. Soc.* **2004**, *126*, 8380.
(31) Zhu, H.; Lan, Y.; Gao, X.; Ringer, S.; Zheng, Z.; Song, D.; Zhao, J. *J. Am. Chem. Soc.* **2005**, *127*, 6730.
(32) Du, G.; Chen, Q.; Han, P.; Yu, Y.; Peng, L.-M. *Phys. Rev. B* **2003**, *67*, 035323.
(33) Wang, R.; Chen, Q.; Wang, B.; Zhang, S.; Peng, L.-M. *Appl. Phys. Lett.* **2005**, *86*, 133101.
(34) Howard, C.; Sabine, T.; Dickson, F. *Acta Crystallogr., Sect. B* **1991**, *47*, 462.
(35) Lazzeri, M.; Vittadini, A.; Selloni, A. *Phys. Rev. B* **2001**, *63*, 155409.
(36) Diebold, U.; Ruzycki, N.; Herman, G.; Selloni, A. *Catal. Today* **2003**, *85*, 93.
(37) Asahi, R.; Morikawa, T.; Ohwaki, T.; Aoki, K.; Taga, Y. *Science* **2001**, *293*, 269.
(38) Tian, N.; Zhou, Z. Y.; Sun, S. G.; Ding, Y.; Wang, Z. L. *Science* **2007**, *316*, 732.
(39) Hu, L.; Peng, Q.; Li, Y. *J. Am. Chem. Soc.* **2008**, *130*, 16136.
(40) Burda, C.; Chen, X.; Narayanan, R.; El-Sayed, M. A. *Chem. Rev.* **2005**, *105*, 1025.
(41) Zhou, K. B.; Wang, X.; Sun, X. M.; Peng, Q.; Li, Y. D. *J. Catal.* **2005**, *229*, 206.
(42) Si, R.; Flytzani-Stephanopoulos, M. *Angew. Chem., Int. Ed.* **2008**, *47*, 2884.